Available online at www.sciencedirect.com
ScienceDirect
Mendeleev Commun., 2023, **33**, 138–140

Mendeleev Communications

One-step synthesis of VB_2 powder by epoxy-assisted borothermal reduction of V_2O_5

Evgeniy S. Novoselov, Dmitriy P. Danilovich and Dmitriy D. Nesmelov*

St. Petersburg State Institute of Technology (Technical University), 190013 St. Petersburg, Russian Federation.
E-mail: dnesmelov@yandex.ru

DOI: 10.1016/j.mencom.2023.01.044

Vanadium diboride was directly synthesized by borothermal reduction of V_2O_5 with the addition of epoxy resin as a reducing agent for the low-temperature reduction of vanadium(V) to vanadium(IV), which leads to the gradual removal of oxygen by the formation of CO gas. The slow rate of gas release prevents destruction of green body, which usually occurs during conventional borothermal reduction. This makes it possible to directly obtain VB_2 powder with an average particle size of 200–300 nm without need to prepare intermediate lower vanadium oxides.

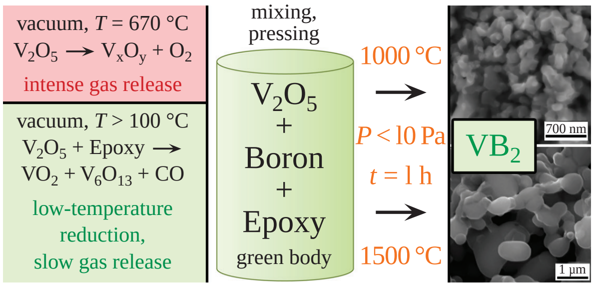

Keywords: vanadium diboride, vanadium oxide, borothermal reduction, epoxy, high-temperature synthesis.

Vanadium diboride is used as a component of high-temperature Fe and Ni alloys, composite refractory ceramic materials and protective coatings on steels. New applications for VB_2 include the development of novel battery electrodes, catalysts for hydrogen fuel cells and other catalytic processes.[1–8] As a component of LnB_6–VB_2 ceramics (where Ln = La, Ce and other rare earth metals) or directionally-crystallized composites, vanadium diboride provides thermionic current density $j = 33.6$ A cm^{-2}, which is much higher than that in traditional LaB_6 cathodes ($j = 4.9$ A cm^{-2}).[9] To create materials based on VB_2 by powder metallurgy, a highly dispersed powder of high purity is required. Traditional high-temperature methods of VB_2 synthesis by direct interaction of elements,[10] as well as carbothermal, borothermal and boron carbide reduction of vanadium(III) oxide,[11,12] lead to the formation of highly pure, but large boride particles ($d > 10$ μm), sintered into high-strength agglomerates. The recently developed low-temperature methods (mechanochemical, synthesis in salt melts, *etc*.) make it possible to obtain VB_2 in a highly dispersed state,[5,15–19] but complex purification of the product from impurities is required. High-temperature methods are still used for large-scale production and their improvement allows one to obtain a highly dispersed powder. Thus, VB_2 with a particle size of 100–800 nm was obtained by reducing V_2O_3 with a mixture of B_4C and C in an argon flow at 1500 °C.[20]

In all the works mentioned above the syntheses of VB_2 have been carried out by reduction of V_2O_3, though V_2O_5 is the most commercially available among vanadium oxides, its cost for 1 kg with the same purity being 8–10 times lower. Difficulty of the direct synthesis of VB_2 from V_2O_5 is due to the two main factors. The first is the partial decomposition of V_2O_5 into V_2O_3, VO_2, and V_5O_9 with heating in vacuum.[21,22] However, V_2O_9 molecules were not detected in the vapor.[23,24] In this case, the large release of oxygen, which leads to the destruction of the compacted V_2O_5–B green body, is the most important issue rather than the specific stoichiometry of the oxides.[21,22] The second factor is the low melting point of V_2O_5 (T_m = 670 °C). The melting of vanadium(V) oxide, which has not decomposed to vanadium(III) oxide, is accompanied by intense evaporation, which also leads to the destruction of the green body. This is usually avoided by carrying out a two-step synthesis with preliminary reduction of V_2O_5 to V_2O_3, which significantly complicates the VB_2 technology.

In this work, the direct one-step synthesis[†] of vanadium diboride by reduction of V_2O_5 and method for suppression of the

---

[†] The preparation of VB_2 was carried out using powders of V_2O_5 (⩾ 99.4 wt%) and amorphous boron (⩾ 99 wt%) with the addition of epoxy resin ED-20 (mass fraction of epoxy groups ⩾ 20.0–22.5%) as a carbon source and binder.

The decomposition of V_2O_5 under 0.1–10 Pa was studied with the addition of 0–10 wt% epoxy resin. The theoretical concentration of epoxy groups was determined as 8% by calculating the amount of carbon residue after the pyrolysis of epoxy resin, which can react with V_2O_5 reducing it to VO_2 (as an average of the sum of lower oxides). Pure V_2O_5 powder and mixture of V_2O_5 with epoxy resin were compacted into briquettes, placed in a graphite crucible and heated in a vacuum electric furnace to 750 °C at a rate of 100 °C h^{-1}, then cooled to room temperature at a rate of 400 °C h^{-1}.

For the one-step preparation of VB_2 the initial components were weighted in stoichiometric quantities according to the reaction:

$$2V_2O_5 + 18B \rightarrow 4VB_2 + 5B_2O_3. \tag{1}$$

The components were mixed in isopropanol media using a vibratory ball-mill with ZrO_2 balls for 24 h, vacuum dried at 50 °C and the compacted green bodies were obtained by uniaxial pressing. Heat treatment of the green bodies was carried out in graphite crucibles in a vacuum electric resistance furnace at 1000 °C and 1500 °C under residual gas pressure of 0.10–10 Pa with a holding time of 1 h.

The structure, phase and elemental composition of the thermally treated vanadium oxide briquettes and synthesized VB_2 powders were studied by X-ray diffraction (XRD) analysis using a Rigaku Smartlab 3 diffractometer with Cu(Kα) radiation, scanning electron microscopy (SEM) using a Tescan Vega 3SBH apparatus and X-ray microspectral analysis with an Aztec X-Act energy dispersive microanalyzer (Oxford Instruments).

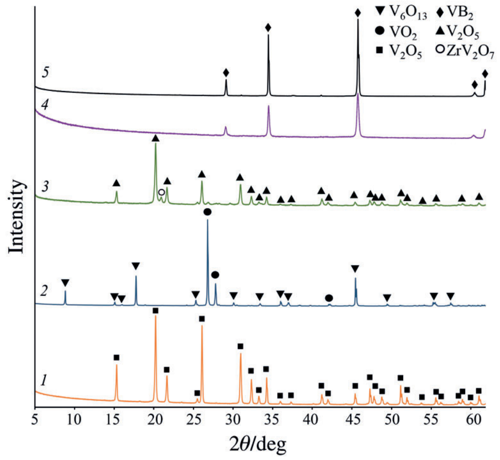

Figure 1 XRD patterns of ‘V_2O_5 + 8% of epoxy groups’ mixture (*1*) before and (*2*) after the heat treatment at 750 °C; V_2O_5 + B + epoxy resin mixture (*3*) before and after the heat treatment at (*4*) 1000 °C and (*5*) 1500 °C.

negative effect of the vanadium(V) oxide decomposition under vacuum are described. The heat treatment of V_2O_5 mixed with 0–10 wt% of epoxy resin at 750 °C under 0.1–10 Pa led to the disintegration of V_2O_5 compacts, contained less than 8 wt% of epoxy resin. An intensive increase in gas pressure was observed at ~670–700 °C (0–4 wt% of epoxy resin). The evolution of gas from mixtures with an epoxy resin content of 5–8 wt% began at 150 °C and increased quite sharply at temperatures up to 670–700 °C. Briquettes of V_2O_5 with the addition of 8–10 wt% of epoxy resin cracked, but retained their shape after heat treatment under the same conditions. No rapid increase in gas pressure was observed in this case. The gradual deterioration of vacuum began at ~100–120 °C. XRD pattern (Figure 1, curve *2*) of the heat-treated ‘V_2O_5 + 8% of epoxy groups’ powder contained reflections of the only two new phases: tetragonal VO_2 and monoclinic V_6O_{13}, which indicates complete decomposition of V_2O_5.

Based on this result, the borothermal synthesis of VB_2 was carried out with 8% of epoxy groups at two different temperatures: 1000 °C and 1500 °C. As expected, no rapid increase in gas pressure was observed during the both experiments. After heat treatment, the samples appeared as loosely bound porous bodies that easily disintegrated in a mortar. XRD patterns of initial and synthesized powders are presented in Figure 1. The initial powder (Figure 1, curve *3*) in addition to the V_2O_5 and boron peaks contains low-intensity reflections of the ZrV_2O_7 impurity phase, which appear as a result of a mechanochemical reaction during ball-milling with ZrO_2 balls. XRD patterns (Figure 1, curves *4*, *5*) indicates complete synthesis of hexagonal VB_2 phase with sharp and intense peaks at 1500 °C and VB_2 with wide peaks at 1000 °C. The difference in the shapes of the peaks is primarily due to the growth of crystallites with an increase in the synthesis temperature (Table 1).

Table 1 Characteristics of the synthesized VB_2.

Characteristics		Synthesis temperature/°C	
		1000	1500
Lattice constants	*a*/Å	3.005 ± 0.005	3.005 ± 0.005
	c/Å	3.070 ± 0.005	3.075 ± 0.005
Crystallite size *d*/nm		73 ± 2	131 ± 2
Average particle size *D*/nm		200–300	800–1000
Element concentration (wt%)	V	68.68 ± 0.02	69.68 ± 0.02
	B	30 ± 2	30 ± 2
	O	1.3 ± 0.5	0.3 ± 0.5
	Zr	0.02 ± 0.02	0.02 ± 0.02

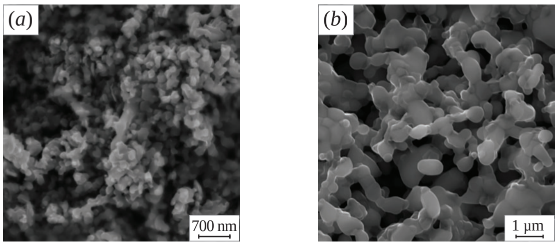

Figure 2 SEM images of VB_2 synthesized at (*a*) 1000 °C and (*b*) 1500 °C.

The lattice constants of vanadium boride are slightly increased compared to the standard. This is due to the impurity of zirconium oxide, which led to the formation of a solid solution. Initial phases are not detected in the XRD spectra of synthesized products. SEM–EDS analysis (Table 1) confirmed the V : B ratio corresponding to VB_2 (within the error of the method). The concentration of oxygen impurities decreases with an increase in the synthesis temperature, which may be associated not only with the completion of the chemical reaction, but also with a decrease in the specific surface area of particles that absorb air oxygen.

SEM-analysis of VB_2 powder [Figure 2(*a*)] indicates that at 1000 °C the average particle size did not exceed 200–300 nm. Increasing synthesis temperature up to 1500 °C [Figure 2(*b*)] leads to the growth of the average particle size up to ~0.8–1 µm. In this case, particles were sintered into low-strength agglomerates with a framework structure.

Thus, the direct borothermal epoxy-assisted synthesis of VB_2 from commercially available V_2O_5 at 1500 °C as well as at a relatively low temperature of 1000 °C leads to formation of a highly dispersed powder of VB_2 with low impurities content.

This work was supported by the Russian Science Foundation (grant no. 19-73-10180).

References

1 S. Licht, S. Ghosh, B. Wang, J. Dianlu, C. Hettige, J. Lau and J. Asercion, *ECS Trans.*, 2011, **35**, 21.
2 M. Lefler, J. Stuart, J. Parkey and S. Licht, *J. Electrochem. Soc.*, 2016, **163**, A781.
3 W. Cai, J. Deng, H. Lu and Y. Cao, *Mater. Chem. Phys.*, 2020, **251**, 123101.
4 S. Licht, C. Hettige, J. Lau, U. Cubeta, H. Wu, J. Stuart and B. Wang, *Electrochem. Solid-State Lett.*, 2011, **15**, A12.
5 F. Wang, M. Wu, B. V. R. Chowdari and Z. Wen, *ACS Appl. Mater. Interfaces*, 2020, **12**, 8219.
6 L. Tian, F. Wang, Z. Zhang and S. Min, *Int. J. Hydrogen Energy*, 2020, **45**, 19017.
7 E. Lee, H. Park, H. Joo and B. P. T. Fokwa, *Angew. Chem., Int. Ed.*, 2020, **59**, 11774.
8 G. Qin, Q. Cui, A. Du, W. Wang and Q. Sun, *ChemCatChem*, 2019, **11**, 2624.
9 S. S. Ordanyan, S. V. Vikhman, D. D. Nesmelov, D. P. Danilovich and I. B. Panteleev, *Adv. Sci. Technol.*, 2014, **89**, 47.
10 R. Kieffer and F. Benesovsky, *Powder Metall.*, 1958, **1**, 145.
11 P. Peshev, L. Leyarovska and G. Bliznakov, *J. Less-Common Met.*, 1968, **15**, 259.
12 V. N. Gurin, *Russ. Chem. Rev.*, 1972, **41**, 323 (*Usp. Khim.*, 1972, **41**, 616).
13 P. Wang, R. Kumar, E. M. Sankaran, X. Qi, X. Zhang, D. Popov, A. L. Cornelius, B. Li, Y. Zhao and L. Wang, *Inorg. Chem.*, 2018, **57**, 1096.
14 J. W. Kim, J.-H. Shim, J.-P. Ahn, Y. W. Cho, J.-H. Kim and K. H. Oh, *Mater. Lett.*, 2008, **62**, 2461.
15 I. I. Korobov, D. Yu. Kovalev, G. V. Kalinnikov, S. V. Konovalikhin, N. Yu. Khomenko, A. A. Vinokurov, A. V. Ivanov and S. P. Shilkin, *Inorg. Mater.*, 2020, **56**, 126 (*Neorg. Mater.*, 2020, **56**, 135).
16 L. Shi, Y. Gu, L. Chen, Z. Yang, J. Ma and Y. Qian, *Mater. Lett.*, 2004, **58**, 2890.
17 Y. Wei, Z. Huang, L. Zhou and S. Ran, *Int. J. Mater. Res.*, 2015, **106**, 1206.

18 Y.-D. Wu, G.-H. Zhang, Y. Wang and R. Xu, *Metall. Mater. Trans. B*, 2019, **50**, 1696.
19 L. Rao, E. G. Gillan and R. B. Kaner, *J. Mater. Res.*, 1995, **10**, 353.
20 Y.-D. Wu, G.-H. Zhang, Y. Wang, R. Xu and K.-C. Chou, *Ceram. Int.*, 2019, **45**, 2492.
21 K. Shibuya and A. Sawa, *AIP Adv.*, 2015, **5**, 107118.
22 M. S. B. de Castro, C. L. Ferreira and R. R. de Avillez, *Infrared Phys. Technol.*, 2013, **60**, 103.
23 E. K. Kazenas and Yu. V. Tsvetkov, *Isparenie oksidov (Evaporation of Oxides)*, Nauka, Moscow, 1997 (in Russian).
24 H. Wang, V. L. Stolyarova, S. I. Lopatin, M. E. Kutuzova and S. Seetharaman, *Rapid Commun. Mass Spectrom.*, 2010, **24**, 2420.

Received: 28th April 2022; Com. 22/6892